[redacted]

NATIONAL ADVISORY COMMITTEE FOR AERONAUTICS

WARTIME REPORT

ORIGINALLY ISSUED
March 1942 as
Memorandum Report

WIND-TUNNEL TESTS OF WICKWIRE-SPENCER PROPELLER

By E. Floyd Valentine and Nicholas Mastrocola

Langley Memorial Aeronautical Laboratory
Langley Field, Va.

NACA

WASHINGTON

NATIONAL ADVISORY COMMITTEE FOR AERONAUTICS

MEMORANDUM REPORT

for the

Army Air Corps

WIND-TUNNEL TESTS OF WICKWIRE-SPENCER PROPELLER

By E. Floyd Valentine and Nicholas Mastrocola

INTRODUCTION

As a result of a request by the Army Air Corps, a propeller submitted by the Wickwire-Spencer Steel Company was tested to determine the aerodynamic properties. The propeller was designed for operation on a small target airplane capable of flying at about 200 miles per hour at 1600 feet altitude with a 175-horsepower engine. The pitch of the propeller is intended to be controlled in flight automatically by forces set up within the propeller itself.

Although the chief object of the tests was to determine the basic aerodynamic properties of the propeller, a few additional tests were made to determine the functional characteristics of the controllable mechanism.

APPARATUS AND METHODS

The tests were conducted in the propeller-research tunnel of the NACA. Figure 1 shows the wing-nacelle combination on which the propeller was mounted. The wing, of NACA 23019.5 section, had a span of 15 feet and a chord of 7.2 feet. All tests were run at zero angle of attack. The radial engine nacelle was 24.5 inches in diameter and was fitted with a perforated plate to simulate the resistance of an engine to the flow through the cowling.

The electric motor used to drive the propeller was overloaded to develop 22 horsepower at 1200 rpm. It was mounted inside the wing and drove the propeller through an extension shaft.

The propeller blades were of laminated wood construction, fitted in metal sleeves to provide rotation within the hub. (See fig. 2.) The tips were metal covered. The blades incorporated an extended trailing edge with a reflex camber over the inner half of the tip radius. This reflex trailing edge was removed for part of the test program. Figure 2 shows the blade form with and without the reflex trailing edge. The blade form curves for both conditions are given in figure 3.

Tests of two methods of pitch regulation were made. For one method the pitch angle assumed by the blades was determined by a balance between the moment of the centrifugal force on the blade-counterweight assembly and a moment applied to the blade roots by the engine torque. In this case the engine torque is applied to a bevel gear which is meshed with gears fastened to the blades in such a way as to tend to turn the blades toward a low pitch position. This gear system also serves the purpose of keeping the two blades at the same pitch. The counterweights were attached to the blade roots in such a manner as to counteract the engine torque and tend to turn the blades in the high-pitch position. The two moments would balance at one rotational speed which would be independent of airspeed or altitude.

In the other method the engine torque is applied in the normal method directly to the hub. The pitch angle assumed by the blades is in this case determined by an equilibrium between the aerodynamic moment of the reflex-trailing-edge blade and the moment of the centrifugal force of the counterweights. Idling gears are used to insure that the blades will each be at the same pitch at all times.

Tests were made with the blades locked at several pitch settings of from 10° to 35° to obtain the basic aerodynamic characteristics of the propeller with both blade forms. The method of running these tests was to increase gradually the tunnel velocity with the rotational speed held constant at its maximum value until the tunnel speed reached its maximum value of 100 miles per hour. The remainder of the desired V/nD range was obtained by reducing the rotational speed. This same method was used in the functional tests to determine the pitch regulation characteristics of the propeller. In the latter case the above procedure was also repeated in the reverse sequence to obtain the effect of friction.

A bank of total-head tubes was mounted behind the propeller disk to determine the effect of the two reflex trailing edges on thrust distribution. The bank of tubes was supported independently of the model.

RESULTS AND DISCUSSION

The propeller results are presented in the form of the nondimensional coefficients, as follows:

$$C_T = \frac{T_e}{\rho n^2 D^4}$$

$$C_P = \frac{\text{Power}}{\rho n^3 D^5}$$

$$\eta = \frac{C_T}{C_P} V/nD$$

$$C_S = \frac{V/nD}{C_P^{1/5}}$$

where

T_e is the effective thrust, namely, measured thrust plus the body drag measured separately

ρ mass density of air, slugs per cubic foot

n rotational speed, rps

D diameter, feet

V airspeed, feet per second

Also, the slipstream distribution is given in terms of pressure ratio, H/q, where

H is the total pressure and

q is the dynamic pressure, $\frac{1}{2}\rho V^2$

The results are presented in the following figures:

Figure 4	C_T	conventional trailing edge
Figure 5	C_P	conventional trailing edge
Figure 6	η	conventional trailing edge
Figure 7	C_S	conventional trailing edge
Figure 8	C_T	reflex trailing edge
Figure 9	C_P	reflex trailing edge
Figure 10	η	reflex trailing edge
Figure 11	C_S	reflex trailing edge
Figure 12		efficiency envelope comparisons
Figure 13		pressure distribution behind propellers
Figure 14		functional results for automatic operation - engine torque versus centrifugal force
Figure 15		aerodynamic characteristics of propeller when in automatic operation - engine torque versus centrifugal force
Figure 16		functional results for automatic operation - aerodynamically stabilized blades

<u>Aerodynamic tests</u>.- As one method of automatic pitch control required the presence of reflexed trailing edges, it was desirable to determine the penalty imposed by this additional portion of the blades. Tests were made, therefore, with the reflexed trailing edges intact, and also with them removed. In figure 12 it may be seen that the propeller was from 1 to 2 percent more efficient with the trailing edges trimmed to conform to conventional practice than with them intact.

As the hub was rather large and not contained within a spinner, a separate drag run was made to determine the effect of the hub on the drag of the body. This hub drag was used in correcting the envelope efficiency curve for the application wherein the hub would be enclosed within a spinner. This correction amounted to from 0 to 2 percent, depending upon the V/nD. The maximum corrected efficiency for the conventional blade form thus reached 85 percent at a pitch setting of 35°. This efficiency is within a percent or so of what would be expected from metal blades.

As the reflex trailing edges are intended to provide a nearly constant or zero aerodynamic moment about the center of rotation of the blades, they must create a drag force at the trailing edge. It would be expected, therefore, that this drag force would result in a loss in thrust. In figure 13 are plots of the pressure distribution in the slipstream for both types of blades. It may be noted that the reflex trailing edge did result in a loss in thrust, particularly for the lower pitch settings. At 15° the entire thrust was concentrated at the outer half of the blades, where no reflex existed, for the propeller with reflex trailing edges; whereas it was concentrated nearer the center of the blades for the propeller with conventional trailing edges.

<u>Functional tests</u>.- In figure 14 are shown plots of power coefficient obtained with automatic pitch operation for the propeller employing torque and centrifugal force as the pitch changing forces. These plots are superposed on plots of power coefficient obtained with the pitch fixed at various angles. It may be noted that with the large counterweights set 10° with respect to the normal of the blade chord line the power coefficient remained fairly constant through a wide range of blade angles. The total variation in power coefficient was only 6 percent for a 15° pitch change, indicating that the engine speed variation would be only 2 percent. For smaller pitch changes, as is contemplated, the power coefficient and engine speed could be held nearly constant. Of further interest is the fact that either a decreasing or increasing power coefficient may be obtained by adjusting the weight, which may be useful for compensating for the loss or gain in power with altitude for certain installations. It may be further noted that the value of the power coefficient was nearly proportional to the size of the weight used. A small weight provided a power coefficient of approximately 0.04, as against 0.08 for the larger weight.

It should be pointed out that inasmuch as the pitch is controlled by engine power and centrifugal force, the blades will adjust themselves, maintaining a constant rpm for a constant torque or power. The effect of air density and airspeed on this equilibrium rotational speed would be small for normal blade configurations for which the aerodynamic moment is small relative to the moments derived from the engine torque and centrifugal force.

The effect of the reflex trailing edge on the operational characteristics of the propeller designed to operate with torque and centrifugal force was inconsequential, as may be noted by comparison of figures 14(a) and 14(b).

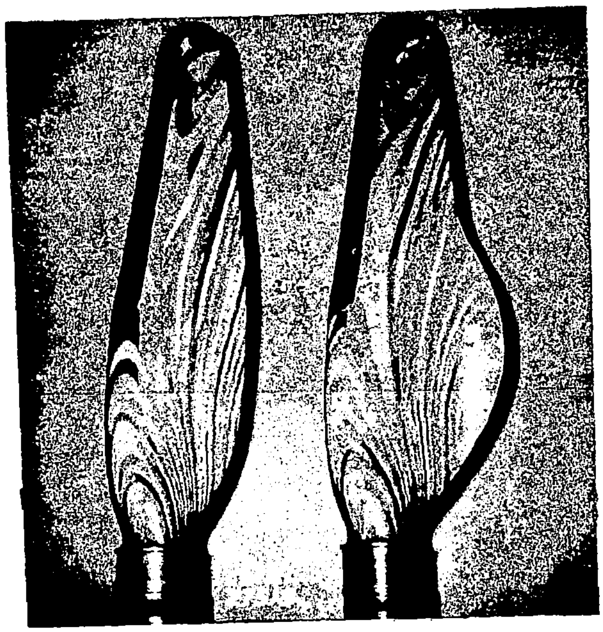

Figure 2.- Propeller blades. Conventional blade and blade with reflex trailing edge.

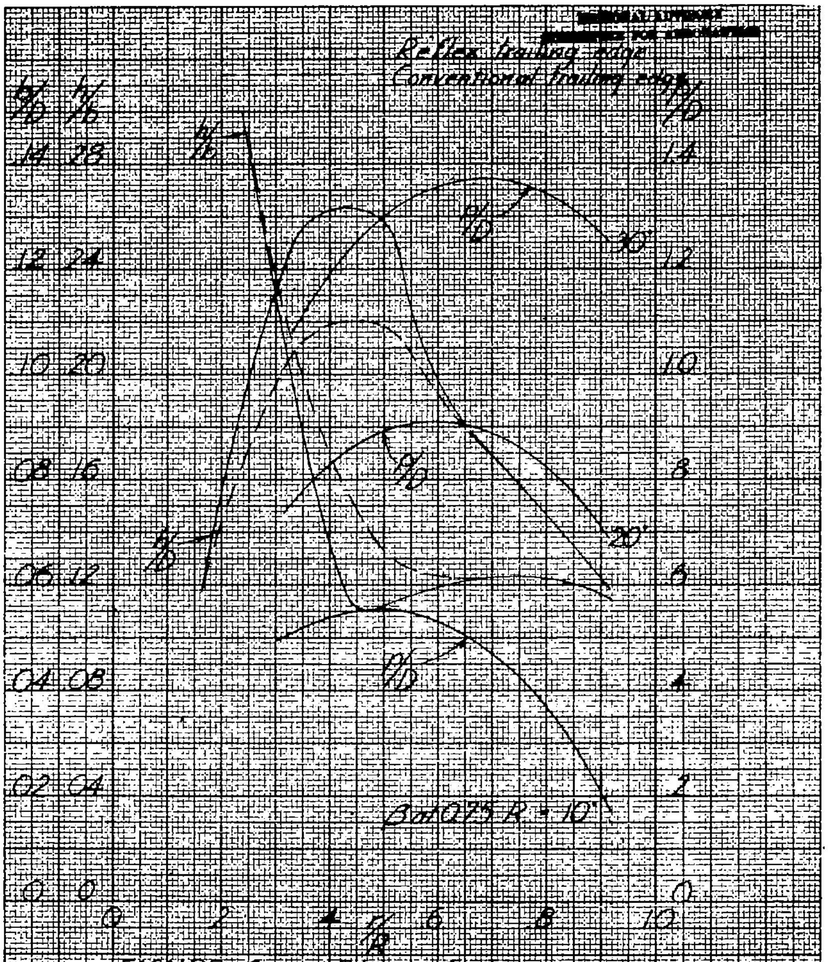

FIGURE 3 — Blade form curves.
b/D, blade width-diameter ratio; p/D, geometric pitch-diameter ratio; h/b, blade thickness ratio.

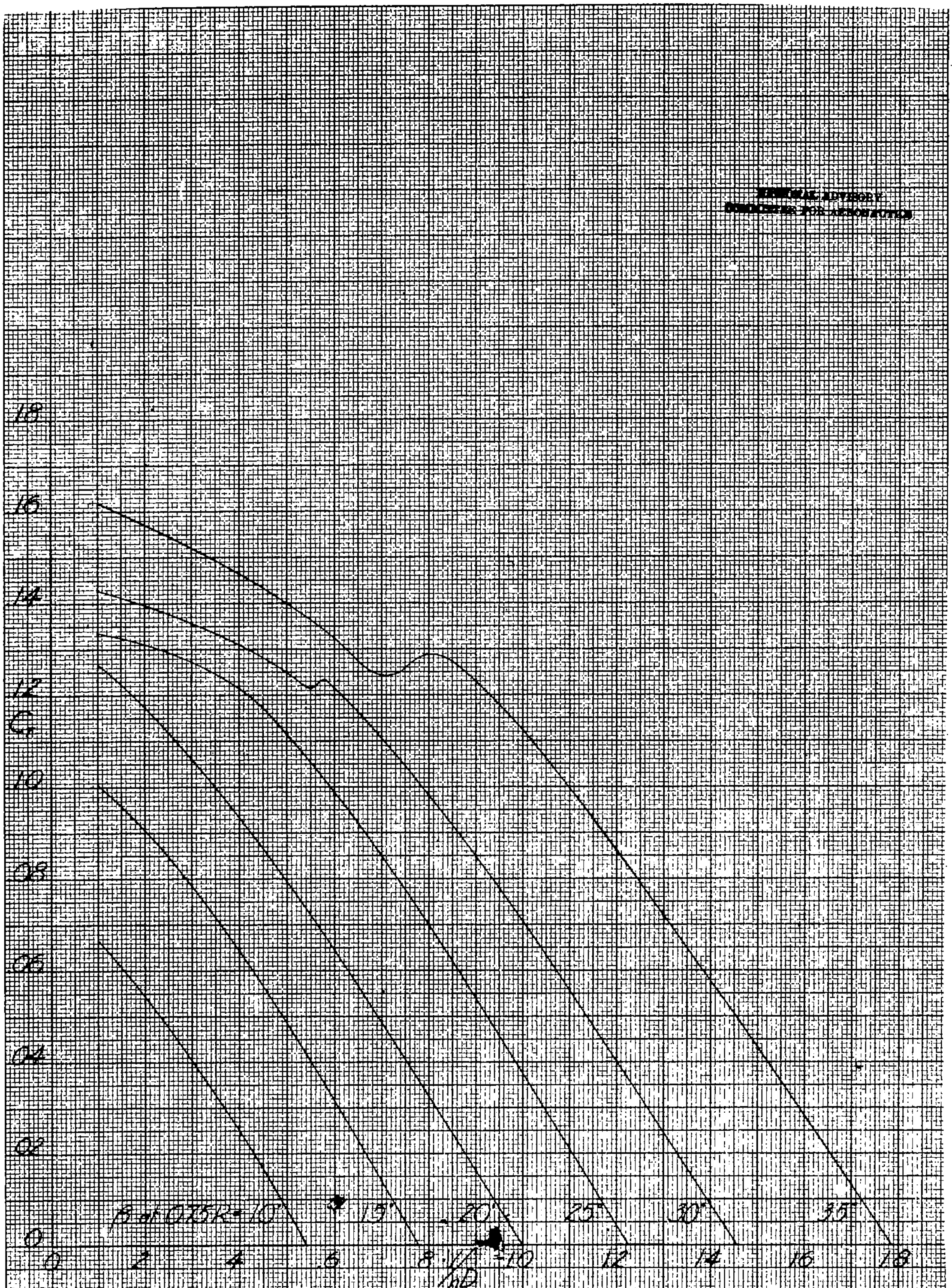

FIGURE 4.– Thrust coefficient curves, conventional trailing edge.

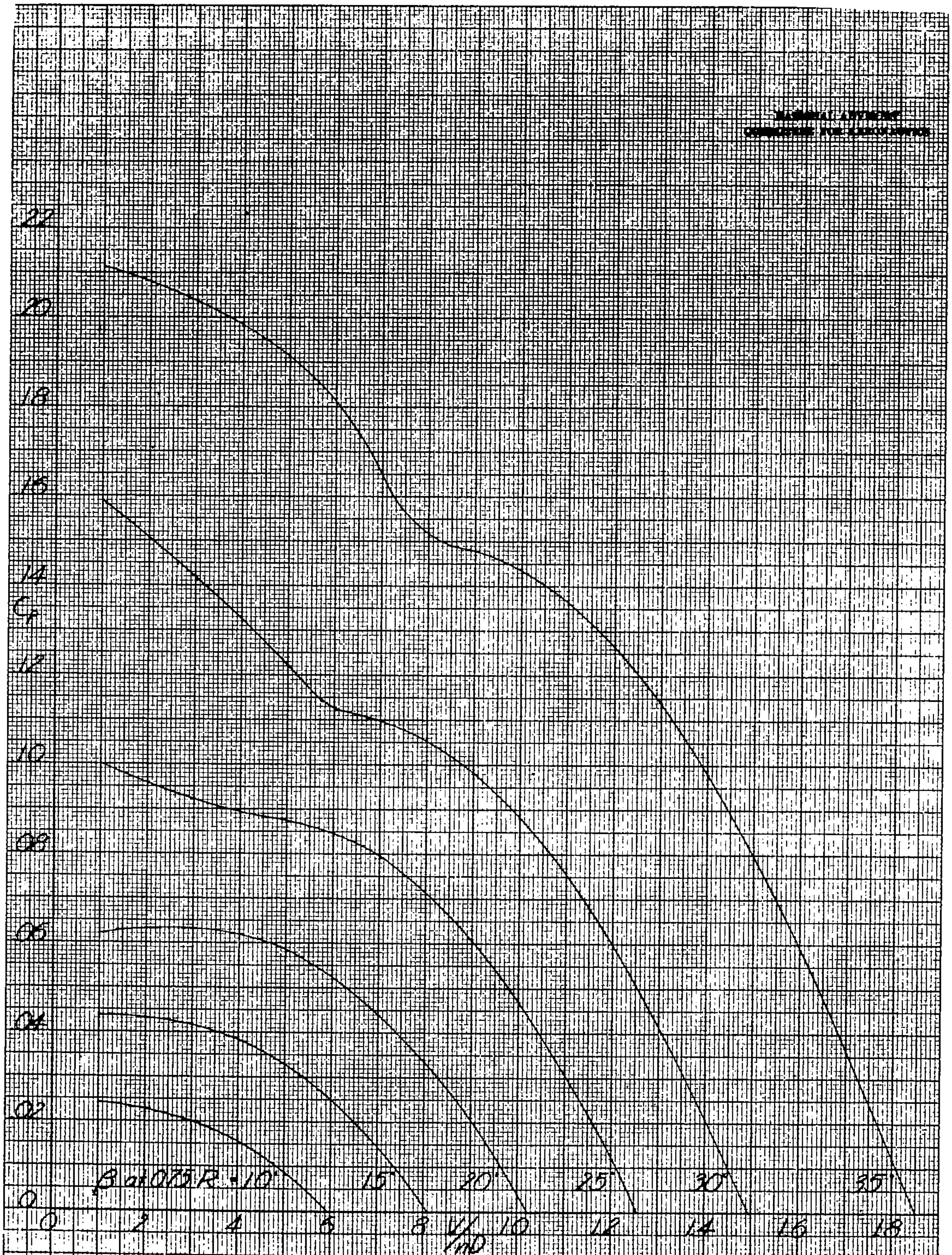

FIGURE 5. – Power coefficient curves, conventional trailing edge.

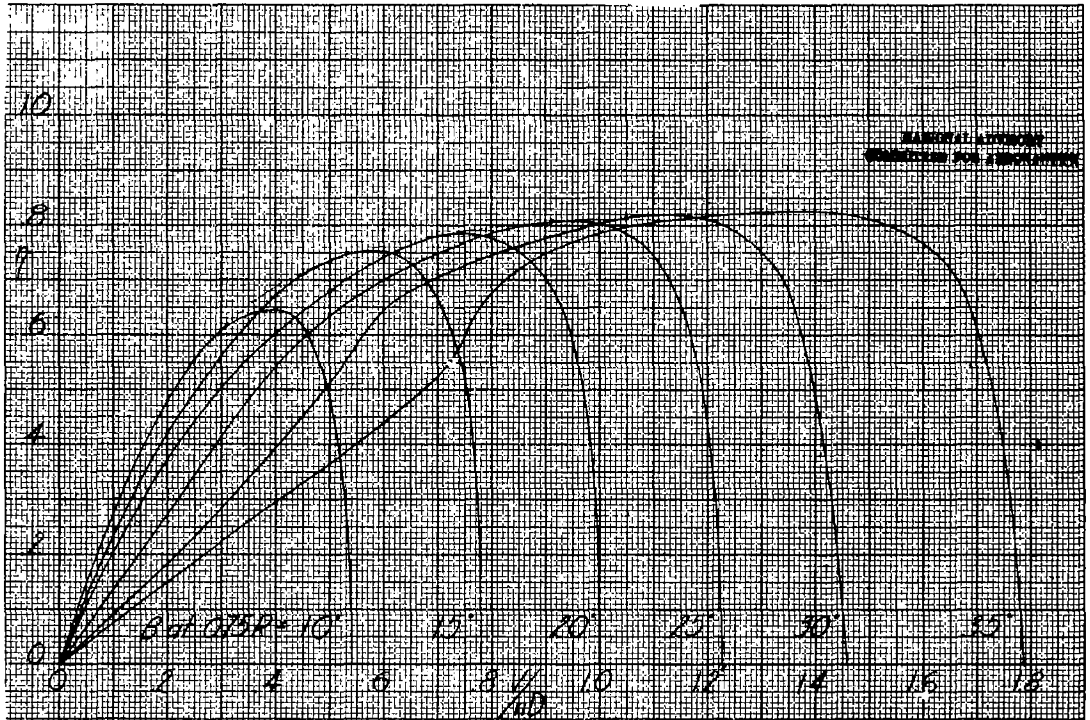

FIGURE 6. - Efficiency curves, conventional trailing edge.

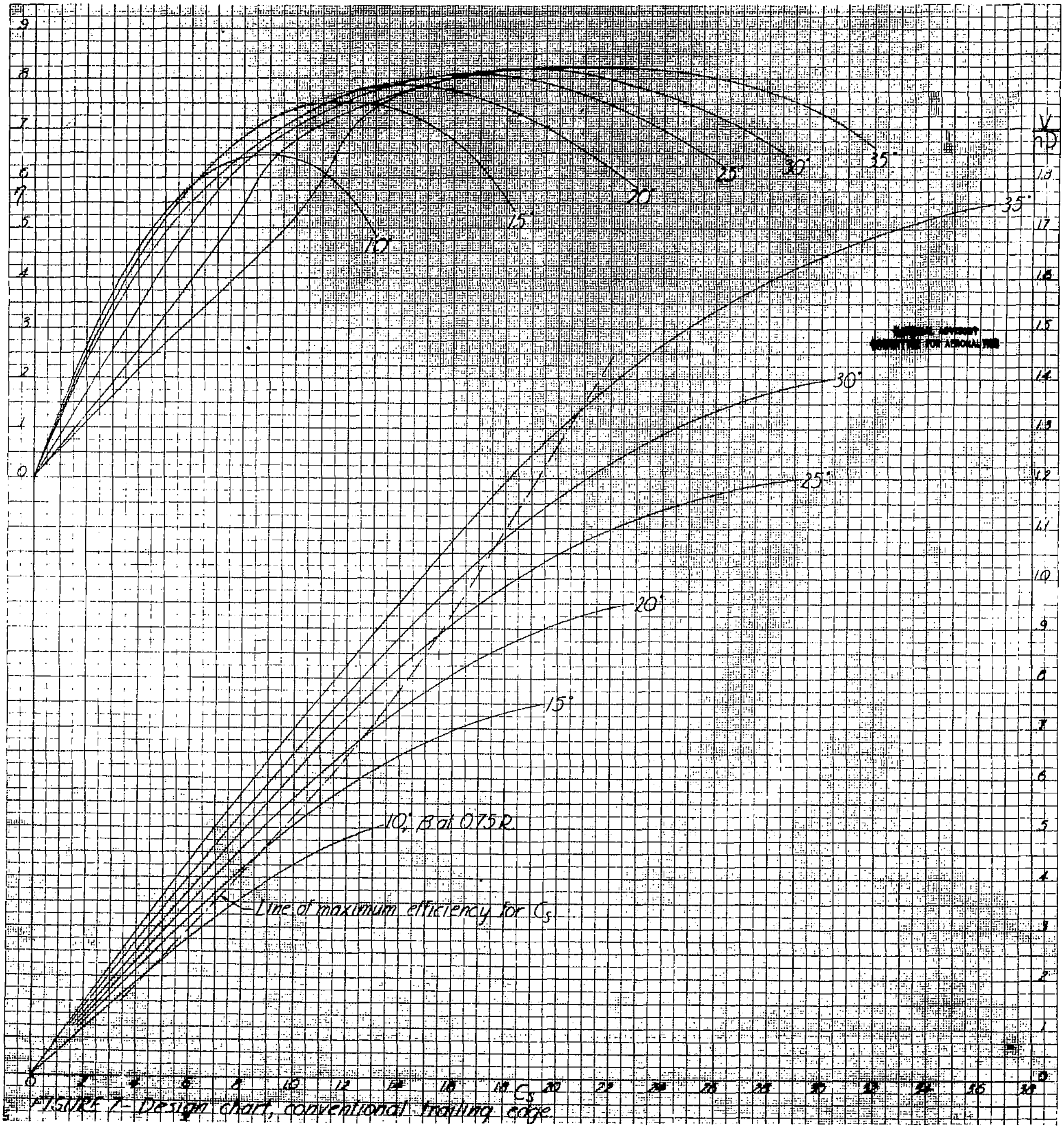

FIGURE 7.- Design chart, conventional trailing edge.

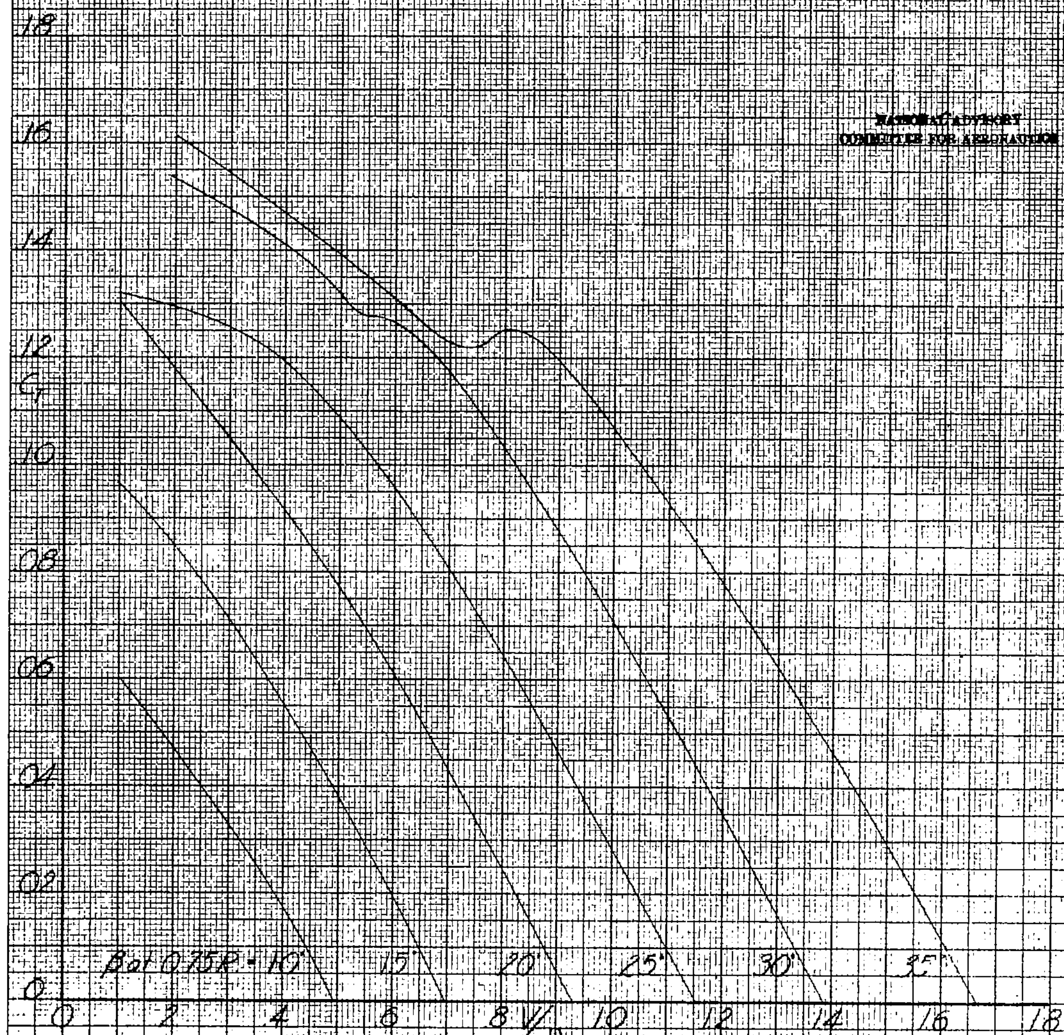

FIGURE 8. – Thrust coefficient curves, reflex trailing edge.

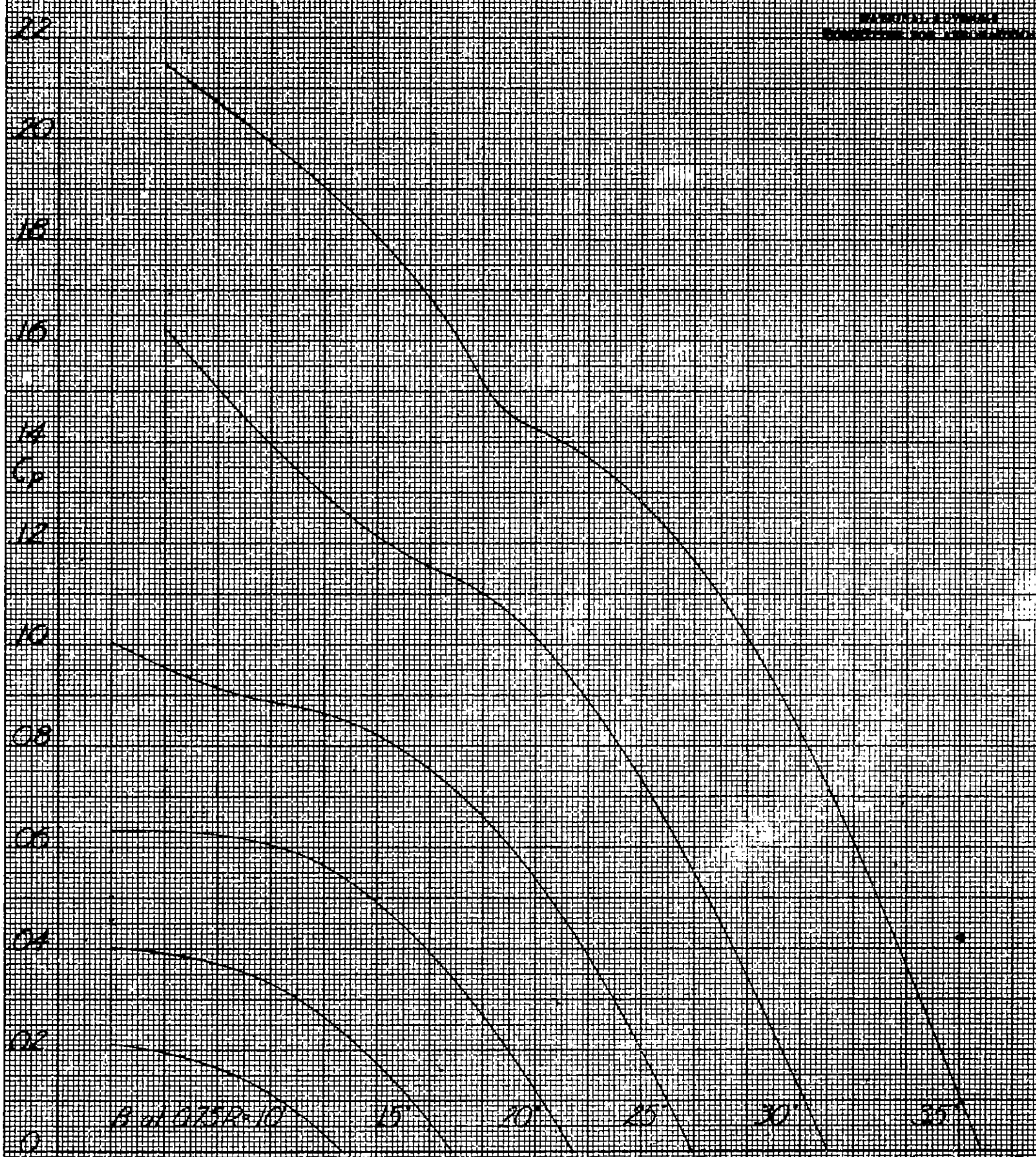

FIGURE 9. — Power coefficient curves, reflex trailing edge.

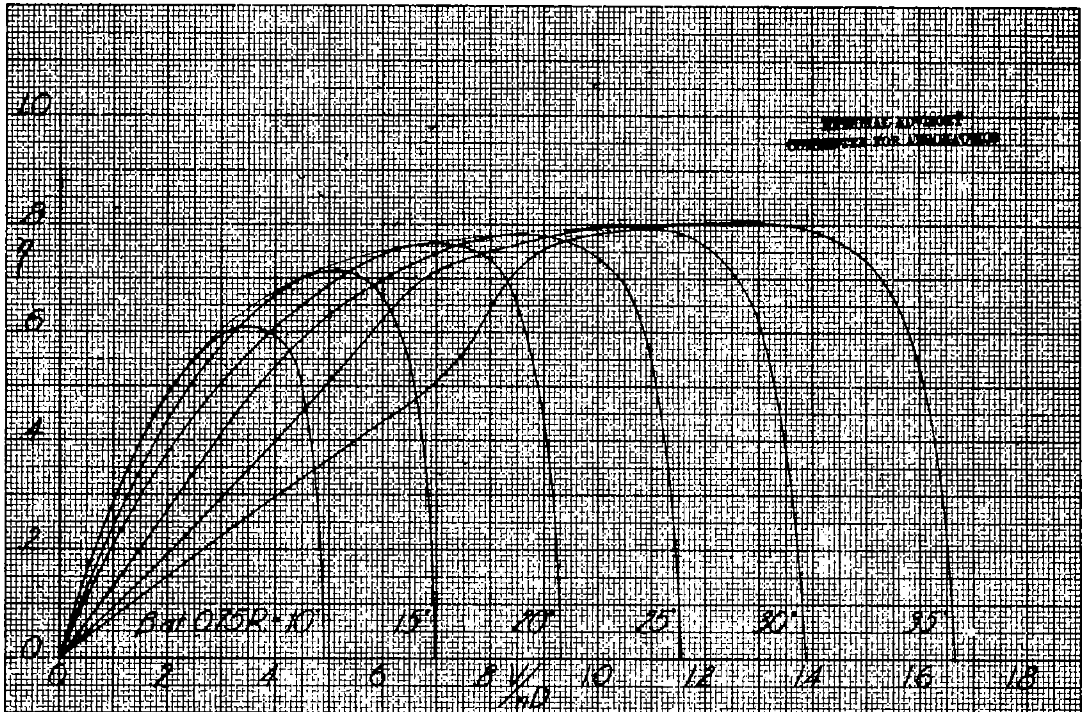

FIGURE 10 – Efficiency curves, reflex trailing edge

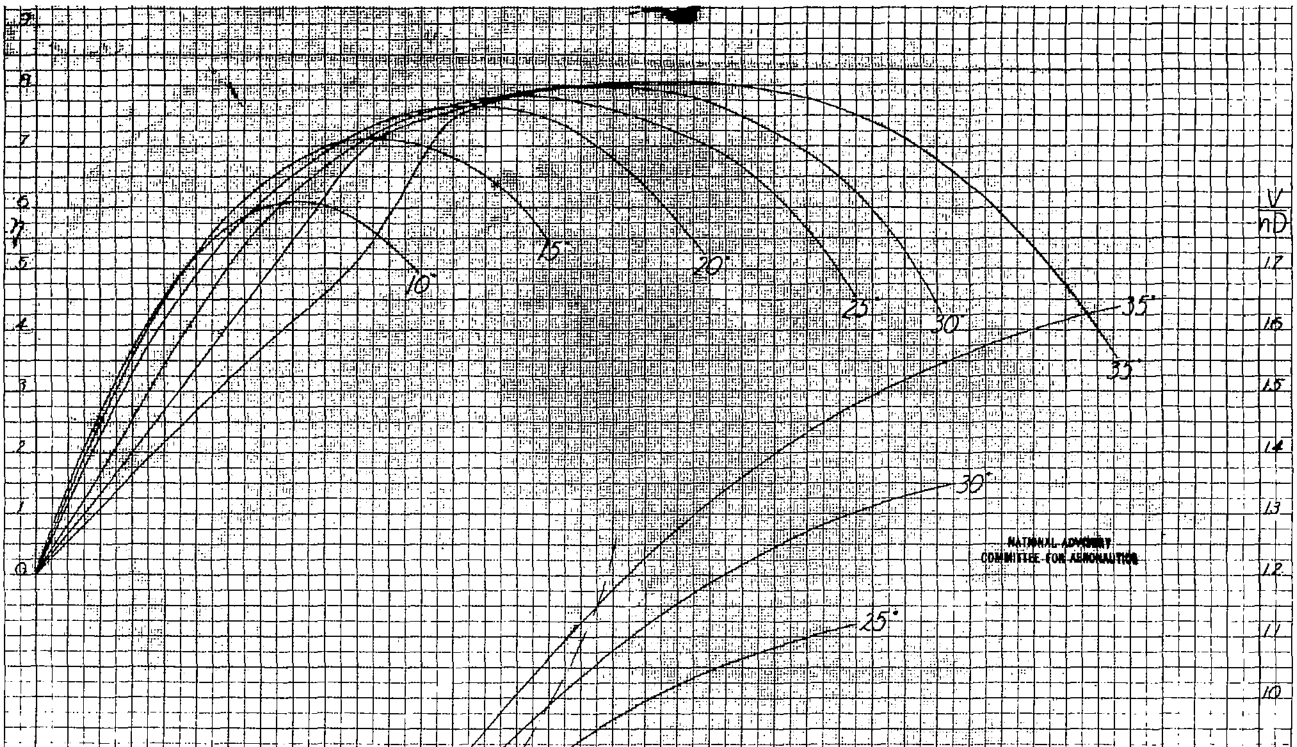

FIGURE 11.- Design chart, reflex trailing edge.

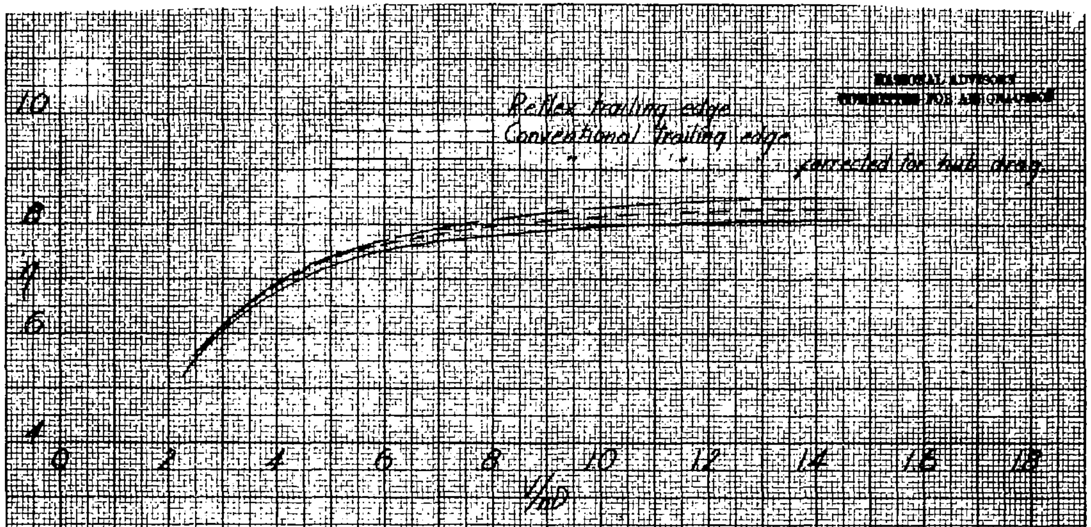

FIGURE 12.- Envelopes of efficiency curves.

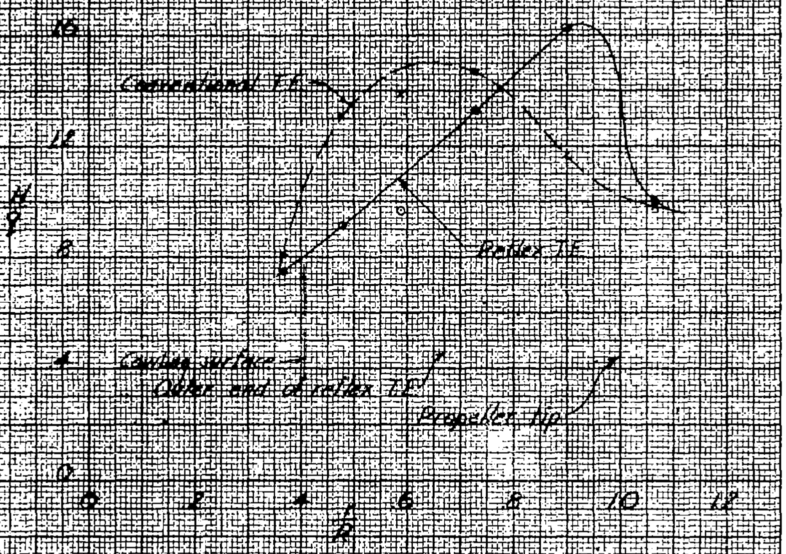

Fig. 13a. Effect of reflex trailing edge on slipstream pressure distribution. β at 0.75R = 15°; V/nD = .388

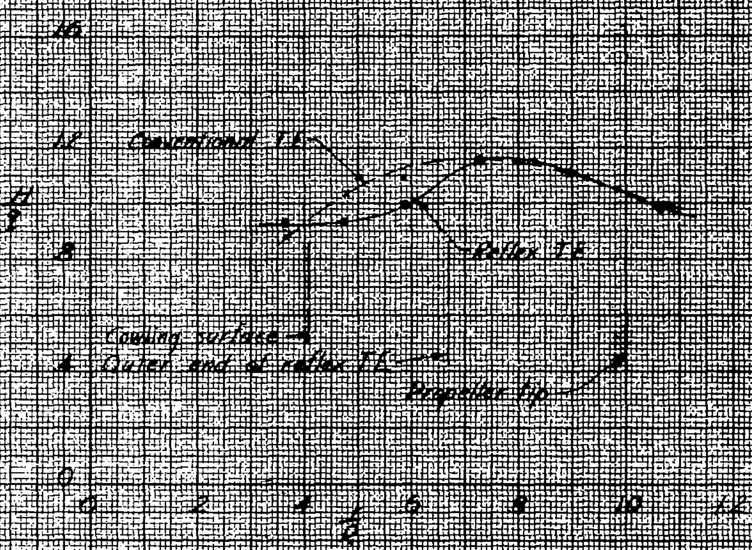

FIGURE 13b.- Effect of reflex trailing edge on slipstream pressure distribution. β at 0.75R = 25°; V/nD = [illegible]

$\beta = 35°$

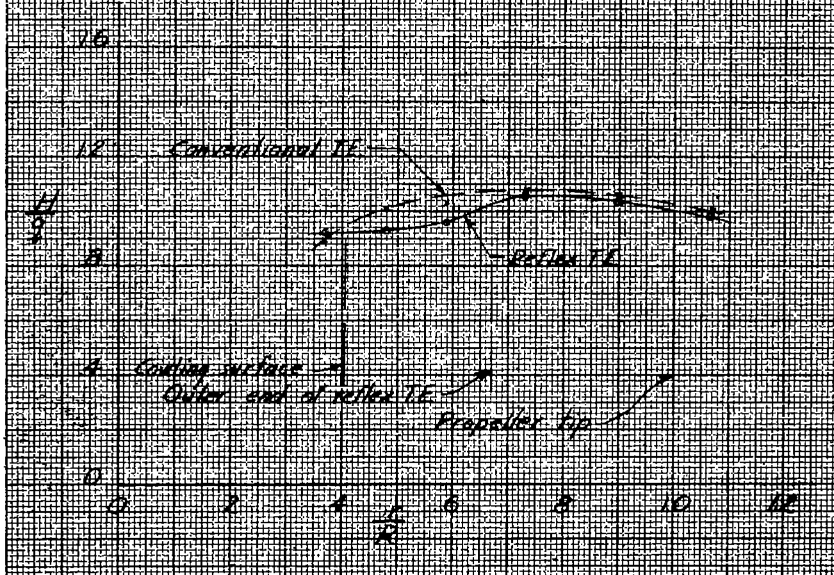

Fig. 13 c. Effect of reflex trailing edge on slipstream pressure distribution, β at 0.75R = 35°, V/nD = 1.54

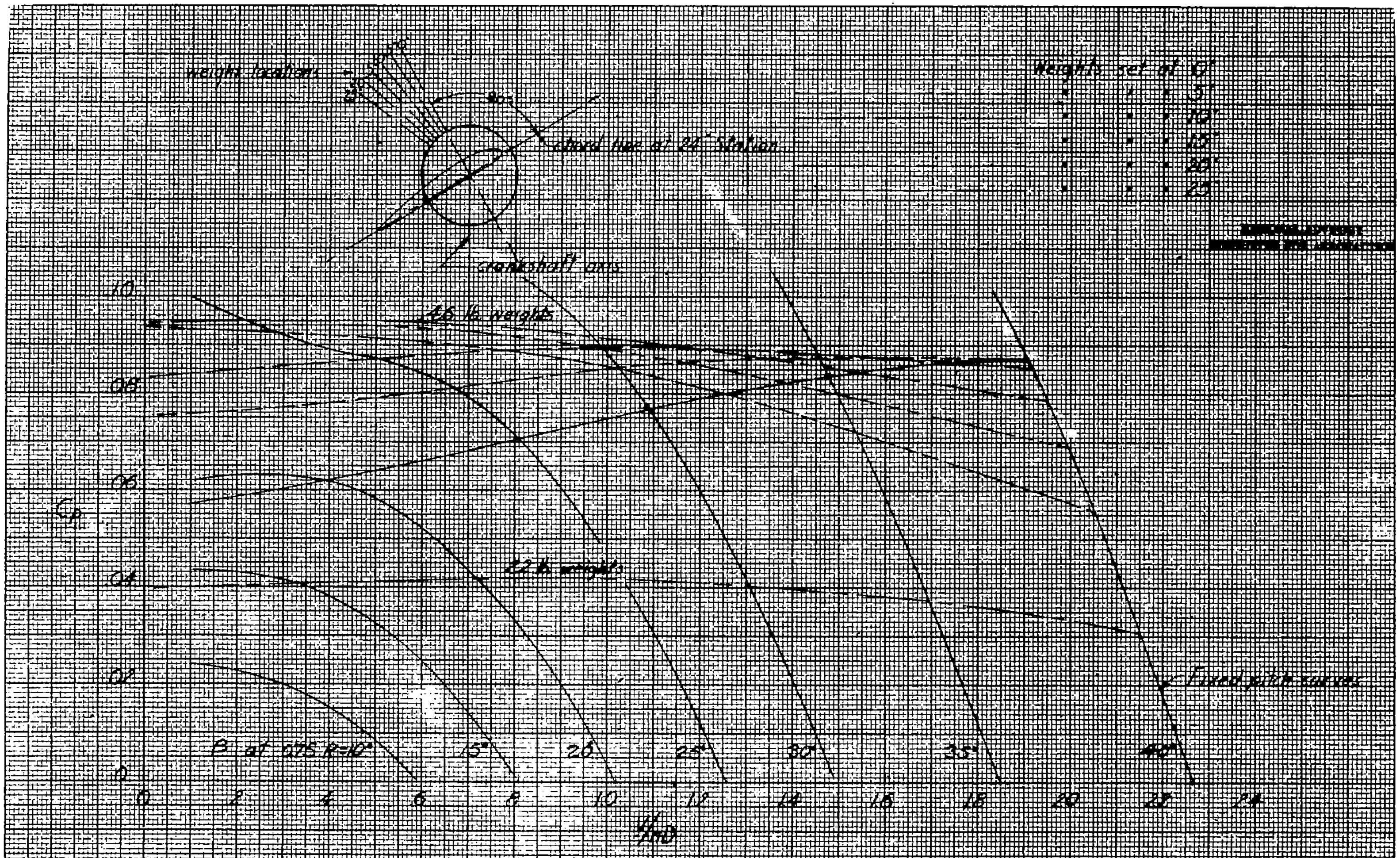

FIGURE 14a.- Functional test of propeller operating with torque and centrifugal force to control the pitch. Conventional trailing edge.

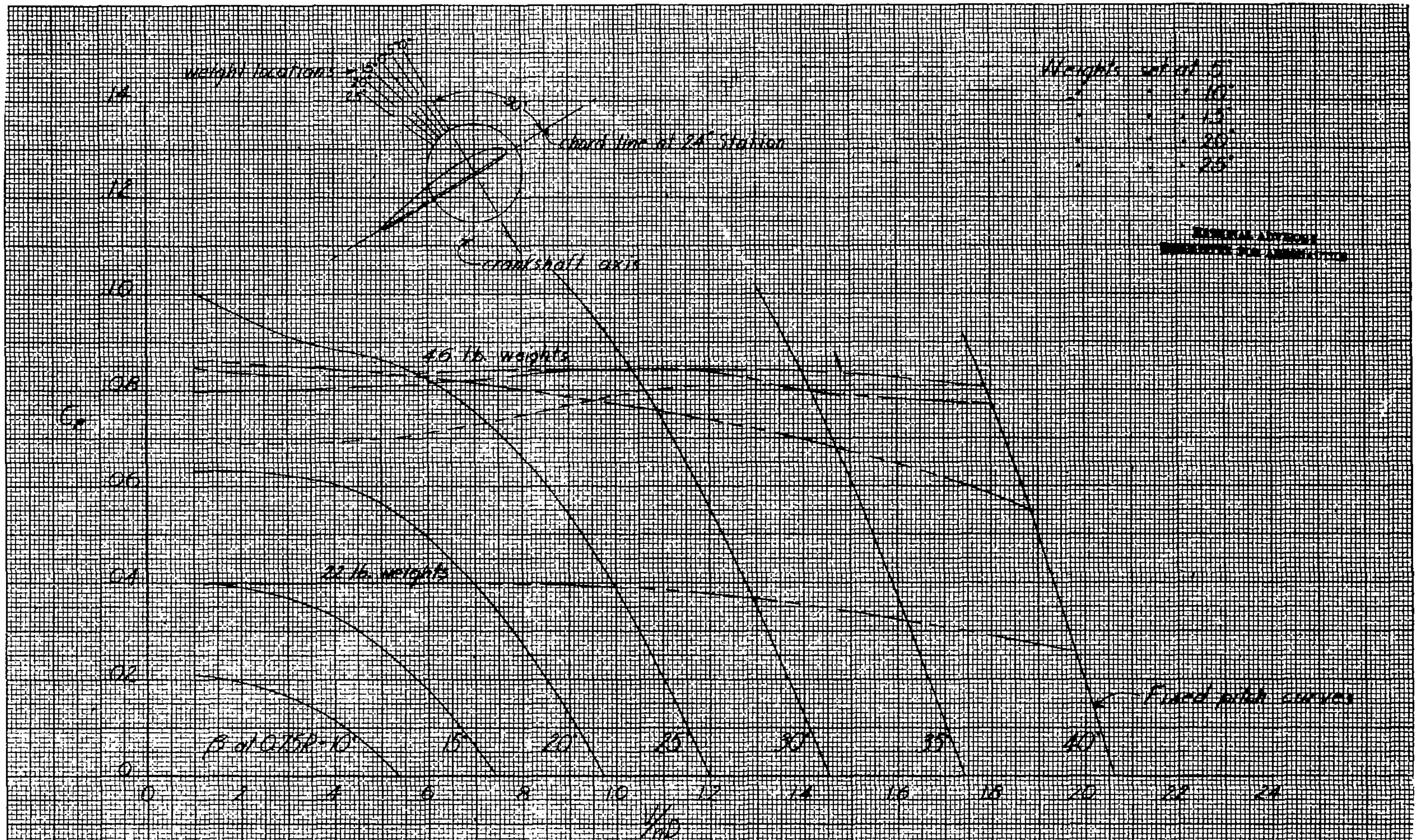

FIGURE 14b.—Functional test of propeller operating with torque and centrifugal force to control the pitch. Reflex trailing edge.

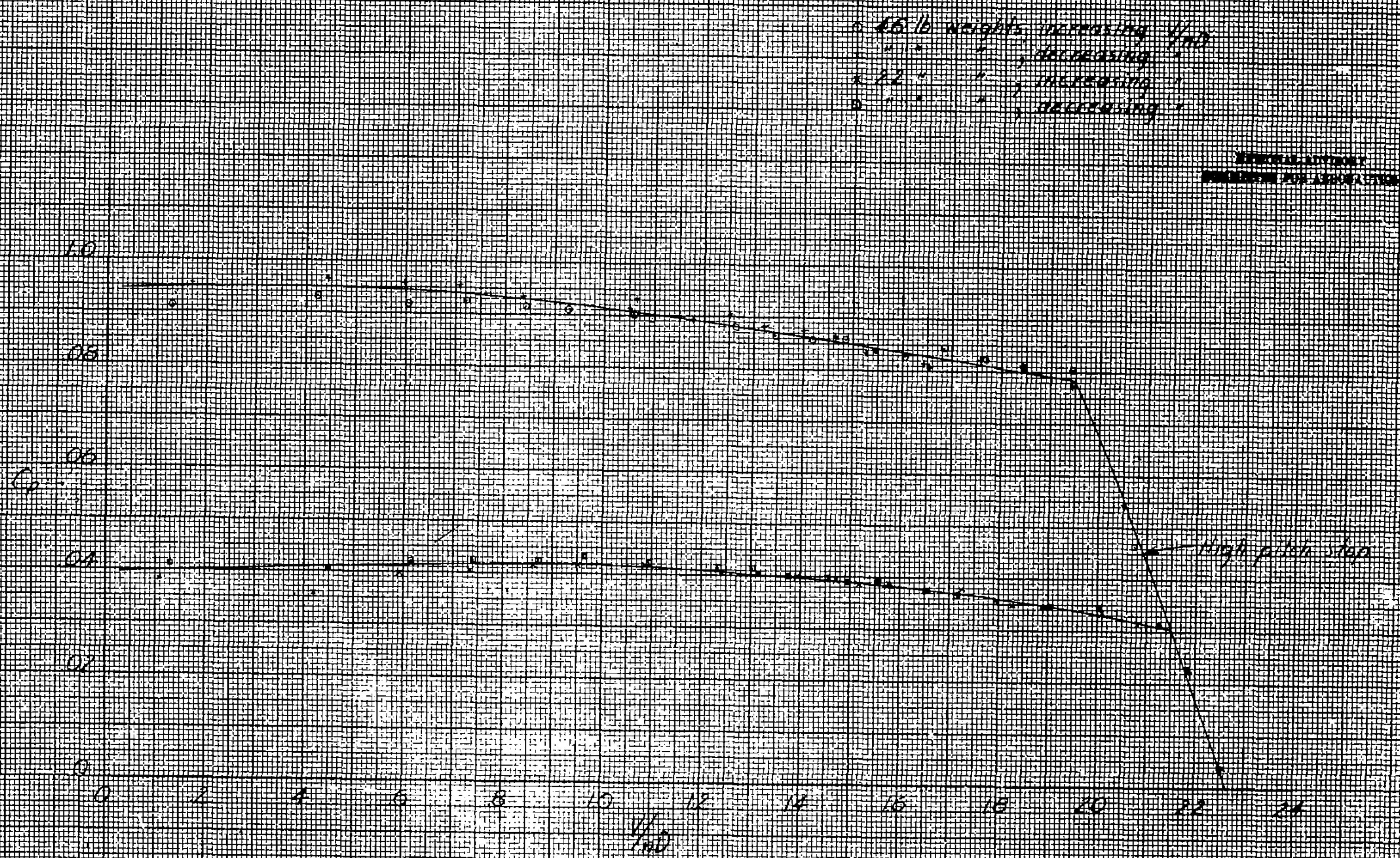

FIGURE 14c.- Effect of friction on automatic pitch control. Balance of torque from centrifugal force on counter weights against engine torque, conventional trailing edge.

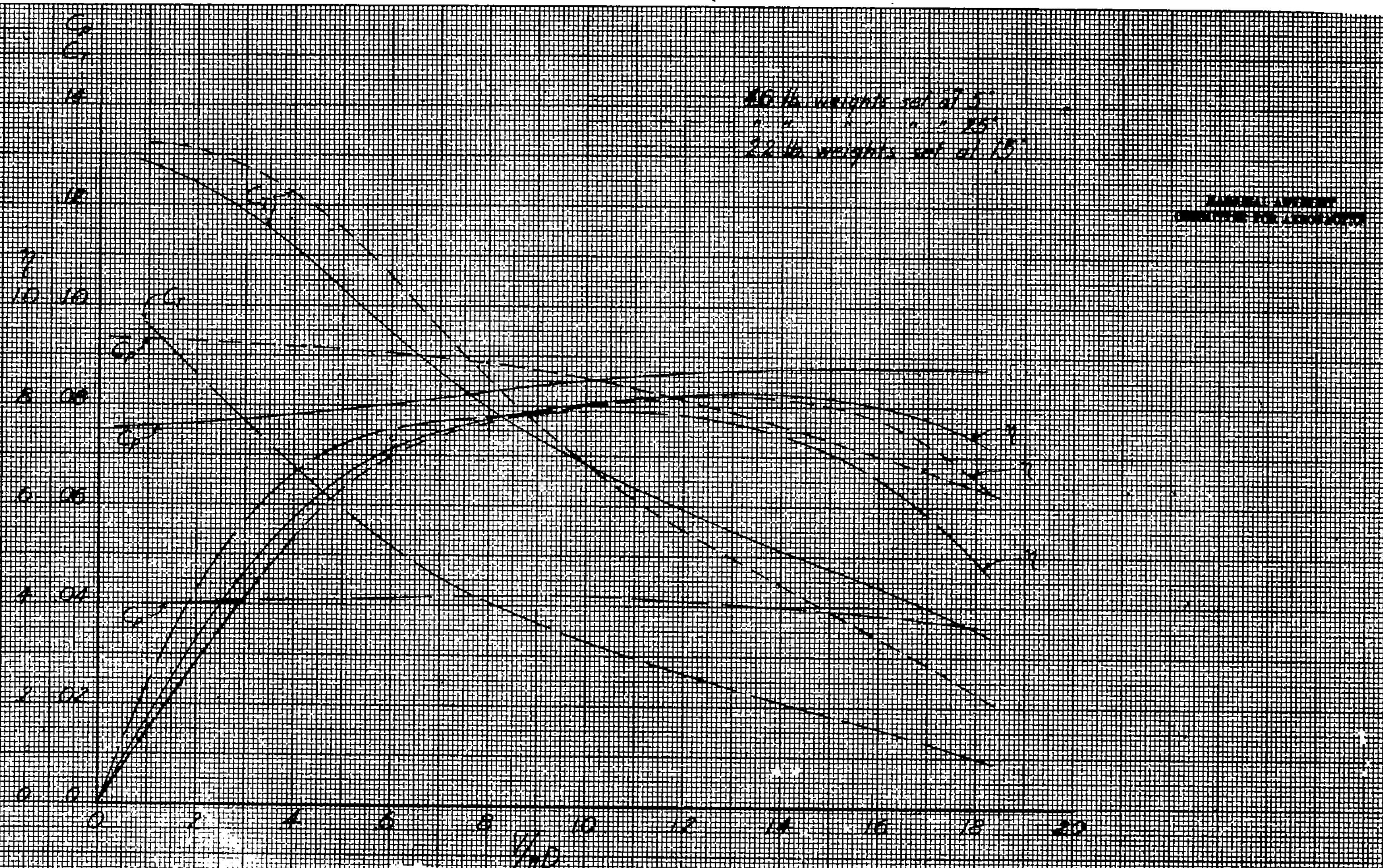

FIGURE 15 Propeller characteristic curves for operation with pitch controlled by torque and centrifugal force. Conventional trailing edge.

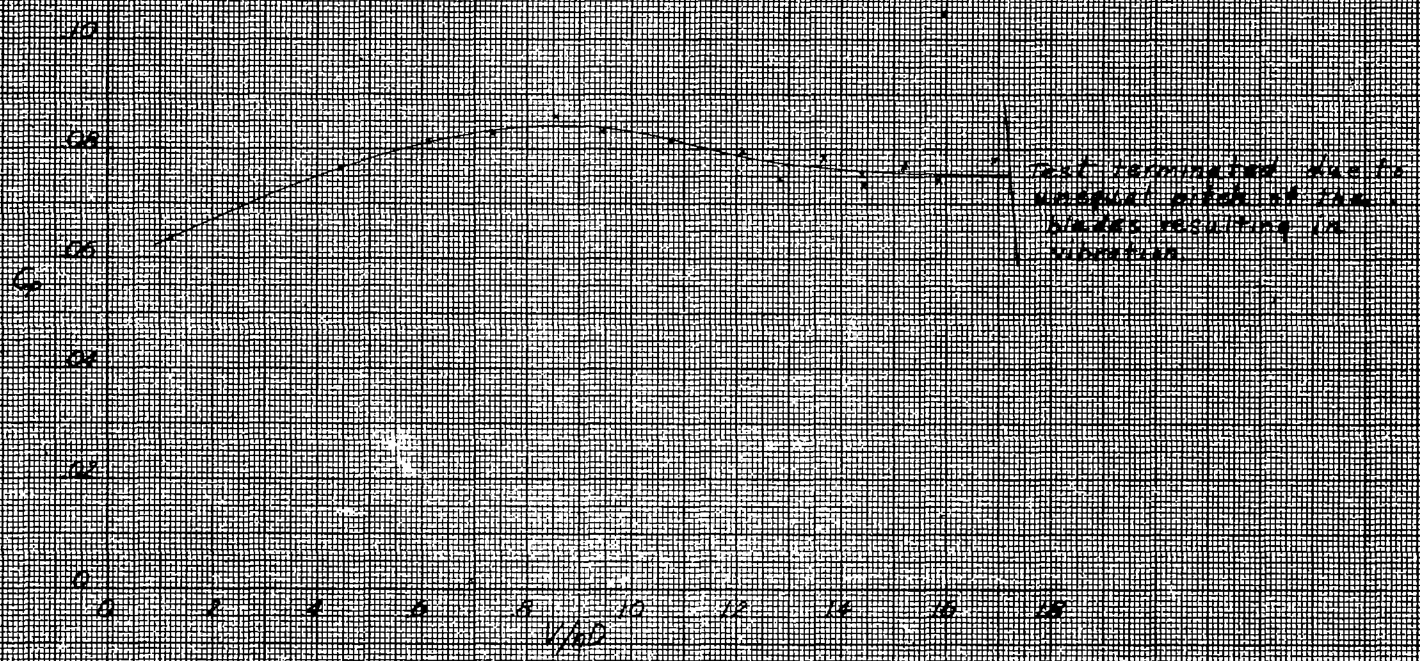

Fig. 15. — Functional test of propeller operating with aerodynamically stabilized blades.